CRACK INITIATION DETECTION and CRACK GROWTH MONITORING WITH DMI TECHNOLOGY

William F. Ranson, Reginald I. Vachon
Direct Measurements, Inc., Atlanta, GA, USA

APPROVED FOR PUBLIC RELEASE, DISTRIBUTION UNLIMITED-DISTAR 11371

INTRODUCTION

This paper presents some of the data on crack detection and monitoring by DMI and Northrop Grumman under a contract between DARPA and Northrop Grumman for the Structural Integrity Prognosis System (SIPS). While several other sensors and vendors are involved in SIPS, this paper focuses on the direct measurements of strain using the DMI technology. For crack detection a baseline reading is made at one point in time, and then subsequent readings of strain are acquired. Crack initiation, detection and crack monitoring are accomplished by taking strain readings periodically over time. An imbalance in strain readings around a hole containing a fastener indicates the presence of cracking, and increasing strain readings can indicate crack growth. Further crack initiation in the barrel of the hole with a fastener is possible prior to the appearance of a surface crack. In either case the theory of the DMI technology is based on the same fundamentals of engineering mechanics. This theory is reviewed and then test results using a two-hole coupon are presented.

THEORY OF DMI MEASUREMENT TECHNOLOGY

First consider that uniform surface strain can be represented as shown by the figure below.

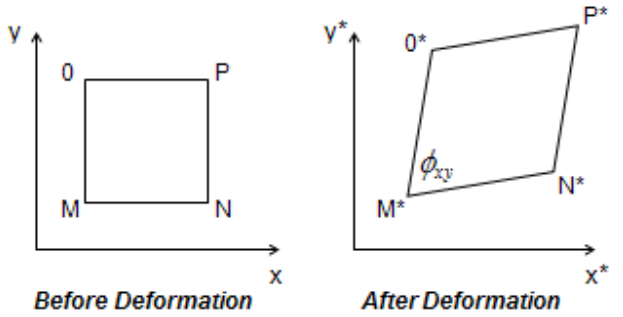

$$E_x = \frac{|M^*N^*| - |MN|}{|MN|}$$

$$E_y = \frac{|M^*O^*| - |MO|}{|MO|}$$

$$E_{xy} = \sin\phi_{xy}(1+E_x)(1+E_y)$$

FIGURE 1. UNIFORM SURFACE STRAIN, WITH ORTHOGONAL AND SHEAR STRAINS

Next consider that non-uniform surface strain can be represented by the figure below.

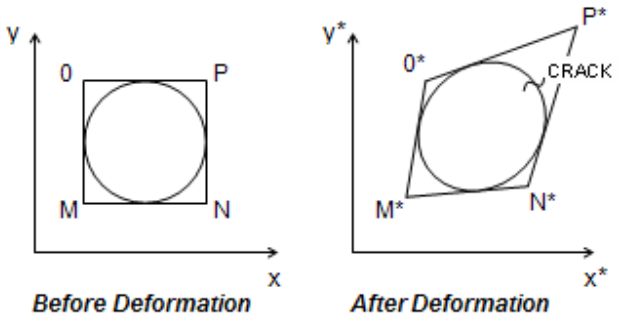

$$E_{MN} = \frac{|M^*N^*| - |MN|}{|MN|}$$

$$E_{NP} = \frac{|N^*P^*| - |NP|}{|NP|}$$

$$E_{MO} = \frac{|M^*O^*| - |MO|}{|MO|}$$

$$E_{0P} = \frac{|O^*P^*| - |OP|}{|OP|}$$

FIGURE 2. NON-UNIFORM SURFACE STRAIN, WITH STRAINS ALONG EACH SIDE

In this latter case (Figure 2) imbalances in strain indicate an anomaly such as crack initiation and/or a crack, and a subsequently increasing imbalance indicates crack growth. Translating the theory as illustrated pictorially and by the equations into a functioning technology is accomplished by representing the elements pictured by a gage in Figure 2 as the set of equations shown in the right-hand side of Figure 2.. Figure 3 shows two views of the DMI gage to illustrate that strain measurements can be made on the outer and inner boundaries of the gage. Further, each gage has a unique number contained in the code between and the inner and outer boundaries. Thus, serialization of DMI gages is possible and they can be numbered from 0 to as high as 4 billion.

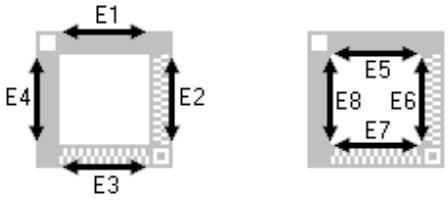

FIGURE 3. DMI GAGE: STRAINS CAN BE MEASURED ALONG INNER AND OUTER BOUNDARIES

The DMI gage is applied to the surface and the gage deforms locally as the surface changes in response to loading. These changes are recorded by the reader, and the data are analyzed by the DMI software to quantify strain. Residual strain represents inelastic deformation. The hardware and software integration for the DMI gage is illustrated in Figure 4. The gage shown in Figure 4 is 10 mm x 10 mm and is scalable to meet application requirements; the handheld reader can also be sized and configured to meet a particular requirement. The verification of the DMI technology to measure strain is based on tests comparing electrical strain gage measurements with DMI strain measurements.

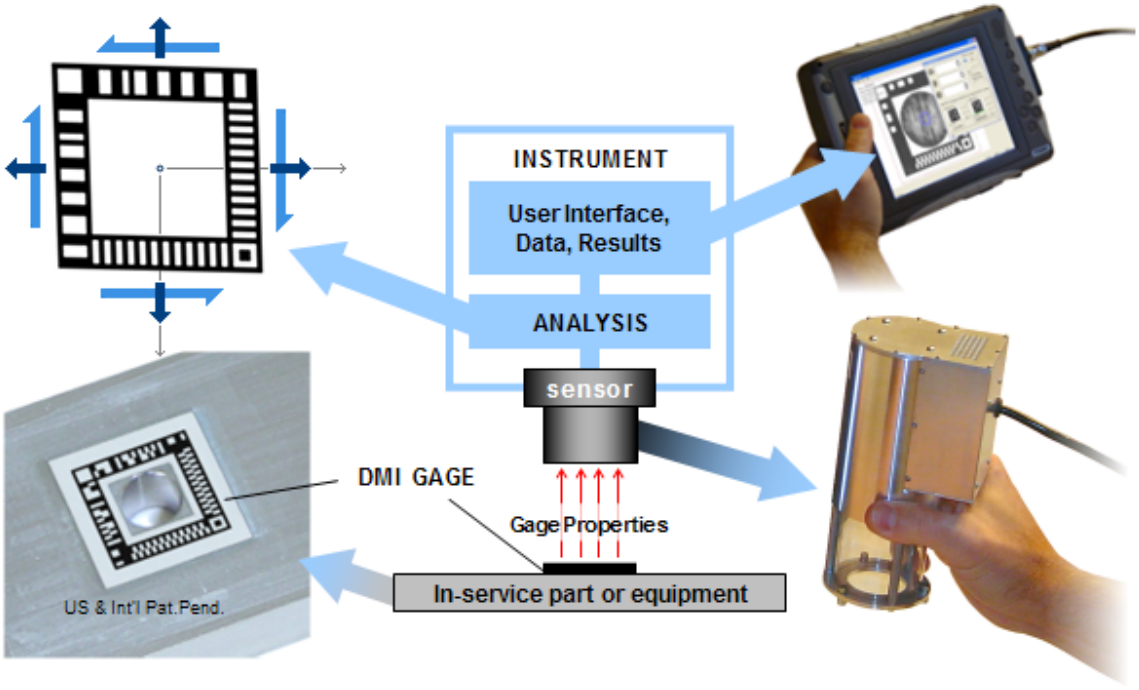

FIGURE 4. DMI TECHNOLGY FOR MEASURING STRAIN

LAB-BASED CRACK DETECTION TESTS

OVERVIEW

DMI has been involved in coupon testing, in support of full scale fatigue tests of two outer wing panels, with Northrop Grumman under the DAPRA SIPS contract cited in the introduction. The material for the coupon testing of holes containing fasteners has been the same as the alloy in the outer wing panels. Specifically, the coupon testing has been conducted at Northrop Grumman using loads and the cyclic loading spectrum very similar to that used on the outer wing panel to provide insight on the full scale fatigue tests. The coupon testing was stopped periodically and strain measurements were made at 40% maximum load to correlate with the procedure associated with the outer wing panel. The coupon tests, while limited in number, provide important insight into the outer wing panel data. Data are not presented on the wing panel tests at this time.

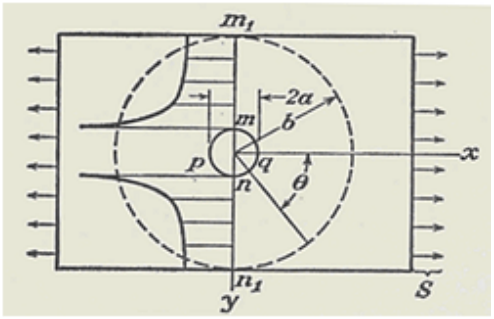

As noted earlier the DMI gage can be queried to yield strain data at the inner and outer boundaries. This is important when using the DMI gage around a hole with or without a fastener. The theory is based on classical mechanics. For example, Timoshenko & Goodier [1] present in the 1951 edition of "Theory of Elasticity" a discussion on the classical solution of the effect of circular holes on stress distribution in plates. The figure to the right presented in [1] illustrates that "the effect of a hole is of a very localized charter." The authors show from Saint-Venant's principle that the change in stress distribution "is negligible at

distances which are large compared with a, the radius of the hole." Thus, the strain near the edge of the hole drops quickly as the distance transverse to the applied load increases. This is an important point, suggesting that strain measurements of the effect of the hole should be made as close to the edge of the hole as possible. This is the requirement for the DMI technology to measure elastic and plastic strain on opposing sides at the edge of a straight-through non-chamfered hole without a fastener. One concludes from theory that a differential in the measurements of strain (if any) on each side of a hole parallel to a load suggests crack initiation, and as the crack grows (on the interior lateral surface of the hole) the differential strain should grow as well. The DMI gage also permits determination of the strain gradient over the distance between the inner and outer boundary of the gage. This provides considerably more strain data to support crack detection. The DMI technology is a practical technique for in-the-field applications as well as research. In this paper, data are presented for the inner and outer boundary of a gage. However, it is interesting to note that the presence of a fastener in a chamfered hole often results in the outer boundary readings of strain being greater than the inner boundary readings. The analytical model for the straight-through hole is different from that for the chamfered hole with a fastener.

COUPON TESTS

DMI conducted tests with Northrop Grumman on a coupon containing two parallel holes. The test coupon was mounted in the cyclic fatigue apparatus with DMI Gage 90 on the left hole and DMI Gage 91 on the right hole in the coupon (Figure 5). Each hole had a fastener. The coupon was subjected to the cyclic loading spectrum used in the later outer wing panel tests. At periodic intervals the cycling was stopped and strain measurements were made on the inner and outer boundaries of each gage. The strain on each boundary is given an alphanumeric identity as shown in Figure 3. The picture on the right depicts the coupon without the fasteners in place prior to testing. The test plan developed by Northrop Grumman and DMI was followed.

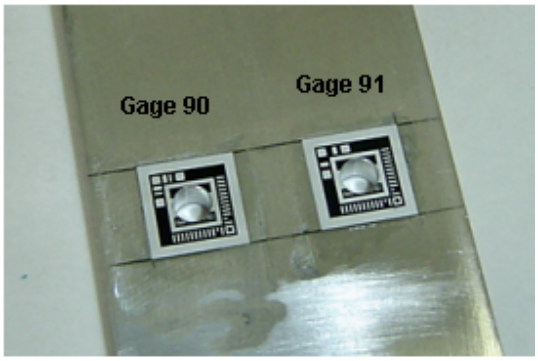

FIGURE 5. TEST COUPON

GAGE 91: Figure 6 shows data collected with the DMI SR-2 technology for DMI Gage 91. The data are seen to be around 1500 microstrain at 40% of the load, corresponding to 40% of the maximum load on the outer wing panel. The data were collected with a fastener in the hole. Data collection from the coupon was stopped at 52,800 cycles because DMI Gage 90 indicated cracks on both sides of the 'left' hole (as described under GAGE 90 results below); however, at this point, Gage 91 was not indicating any cracks in the 'right' hole. When the fatiguing was stopped, the coupon fastener in the 'right' hole was removed, and the Hirox microscope was used to inspect the hole. No cracks were observed. After all testing was completed the coupon was statically overloaded and fractured in half along the diameter of the hole; the fracture picture for Gage 91, shown in Figure 7, supported the findings from the Hirox microscope and the data from Gage 91. The absence of cracks was expected based on previous experience with test coupons, as the data for DMI Gage 91 in Figure 6 show little deviation between the inner and outer boundary readings of strain over time. Thus, there was anticipation as to the indication of cracks from data taken with DMI Gage 90.

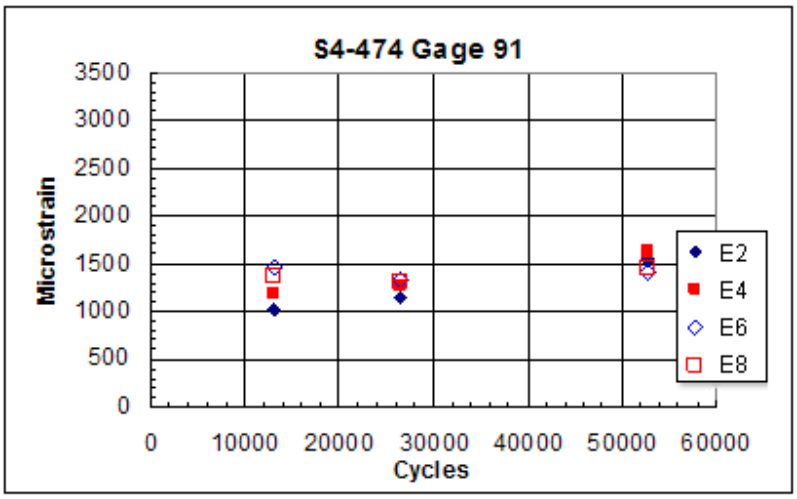

FIGURE 6. GAGE 91 STRAIN vs. CYCLES

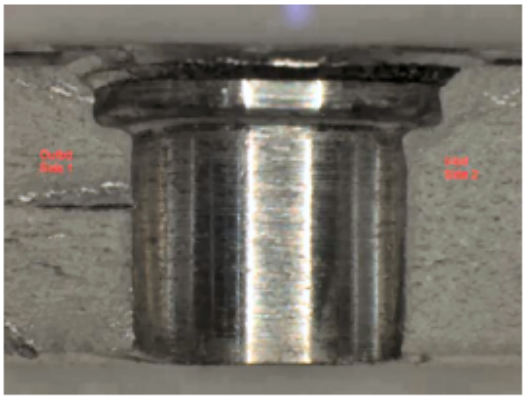

FIGURE 7. GAGE 91 FRACTURE PICTURE

GAGE 90: The data in Figure 8, taken with a fastener in the hole at DMI Gage 90 show considerable deviation in the strain at the inner boundaries of the gage and in the strain at the outer boundaries of the gage between 26,400 cycles and 52,800 cycles. The data at 13,200 cycles and 26,400 cycles show strain around 1500 microstrain which is close to the values measured at Gage 91 up to 52,000 cycles. The deviations in strain for Gage 90 between 26,400 and 52,800 cycles indicated that cracks occurred in the lateral surface area of the hole on both the left-hand and right-hand sides of the hole under Gage 91. This interpretation of data was supported by Hirox observation and fracture pictures. After the strain readings were made at 52,800 cycles, the fastener was removed from the hole under Gage 90 and the Hirox microscope was used to observe the internal lateral surface area. Cracks were seen on both sides of the hole, which supported the indications of the DMI measurements made during testing. The photograph of the fractured coupon is displayed in Figure 9, which clearly shows a characteristic fracture on each side of the hole. The crack initiation in the 26,400 to 52,800 range was not expected based on experience and analyses. The data demonstrated that crack growth could be observed when the strain level exceeded 1500 microstrain.

This conclusion is based on previous data collected by DMI showing that crack initiation can be inferred when the strain readings around a hole are constant and then begin increasing almost linearly from the point of crack initiation. The coupon test provides the strain level beyond which one would anticipate cracking to be observed by this sensor for the material of the outer wing panel of the same alloy, in this case 1500 microstrain.

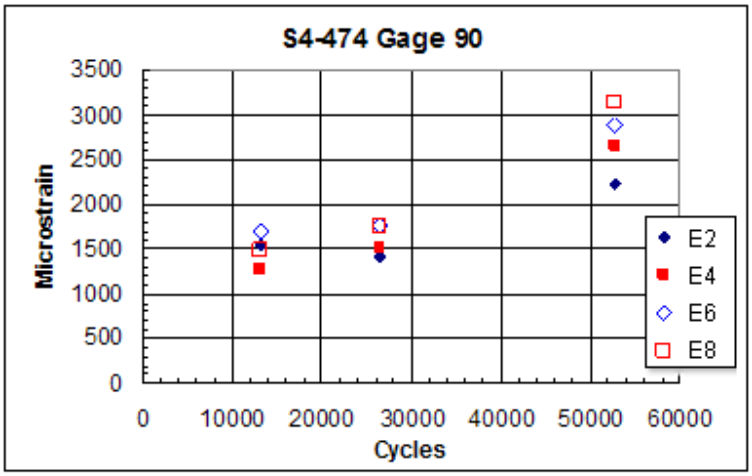

FIGURE 8. GAGE 90 STRAIN vs. CYCLES

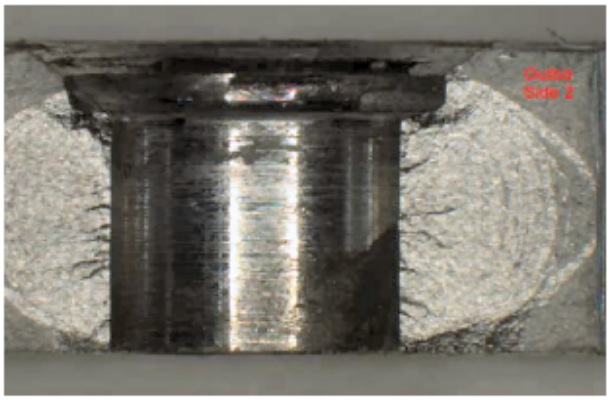

FIGURE 9. GAGE 90 FRACTURE PICTURE

CONCLUSION

One can postulate the following, based on coupon testing:

1. Deviations in strain readings between the left- and right-hand sides of the DMI gage parallel to the direction of the load, as a function of time, indicate crack initiation in the barrel of the hole on the side with the larger strain reading; e.g. if the strain is larger on the right-hand side than the left-hand size of the gage as a function of time, then crack initiation is found to be on the right-hand side of the internal lateral surface of the hole.

2. When cracks form on both sides of the internal lateral surface of a hole with a fastener, the strain readings on both the left-hand and right-hand sides of the DMI gage, parallel to the load, increase compared to data acquired earlier in the measurement.

3. The DMI SR-2 technology can detect crack formation on the internal lateral surface of a hole with a fastener prior to the crack appearing on the external surface adjacent to the hole.

Further, to these conclusions one can also postulate that strain readings on each side, or one side, of the hole may exceed a threshold strain reading for detecting an actual crack, and this would indicate crack initiation in the plastic zone.

REFERENCES

[1] S. Timoshenko and J.N. Goodier, Theory of Elasticity, McGraw-Hill Book Company, Inc. New York, 1951

[2] W. Elber, Fatigue Crack Propagation, Ph.D. Thesis, University of N.S.W., Australia, 1968

[3] W. Elber, Fatigue Crack Under Closure Cyclic Tension, Eng. Frac. Mech., 3,37-34 (1970)

[4] W. Elber, The Significance of fatigue crack Closure, Damage Tolerance in Aircraft Structures, ASTM STP 748, 53-84(1981)

[5] J.C. Newman Jr., M. Jordan Haines, Verification of stress-intensity factors for various middle-crack tension test specimens, Eng. Frac. Mech., 72, 1113-11, (2005)

[6] Kiran Solanki, S.R.Daniewz, Jc. Newman Jr., Finite element analysis of plasticity-induced fatigue crack closure: an overview, Eng. Frac. Mech., 71,149-171 (2004)

[7] S.K. Ray, R Perez, A.F. Grandt Jr., Fatigue and Fracture of Engineering Materials and Structures, 10 (3), 239-250, (1987)

[8] A.I. Rifani, A.F. Grandt,Jr., A FRACTURE MECHANICS ANALYSIS OF FATIGUE CRACK GROWTH IN A COMPLEX CROSS SECTION, Engineering Failure Analysis, Vol 3., No. 4 249-265 (1996)

[9] D. S. Dawicke, A.F. Grandt Jr., and J.C. Newman Jr. THREE-DIMENSIONAL CRACK CLOSURE BEHAVIOR, Eng. Frac. Mech., Vol. 36, No. 1, 11-121 (1990)

[10] J.C. Newman Jr., A. Brot, C. Matias, Crack-growth Calculations in 7075-T7351 aluminum alloy under various load spectra using an improved crack-closure model, Eng. Frac. Mech., 7, 2347-2363 (2004)

[11] Karl-Heinz Schwalbe, Jams C. Newman Jr, John L. Shannon Jr. , Fracture mechanics testing on specimen with low constraint-standardization activities within ISO and ASTM, Eng. Frac. Mech., 72 557-576 (2005)

[12] Dale L. Ball and Mark T. Doerfler, Experimental and Analytical Studies of Residual Stress Field Evolution and Fatigue Crack Growth at Cold Expanded Holes , 2003 USAF ASIP Conference Savannah, GA Dec 2003